Analytical characteristics of a commercial ICP orthogonal acceleration time-of-flight mass spectrometer (ICP-TOFMS)

Sturgeon, R.; Lam, J.; Saint, A.

Publisher's version / Version de l'éditeur:
https://doi.org/10.1039/b000496k
Journal of Analytical Atomic Spectrometry, 15, 6, pp. 607-616, 2000

JAAS

Full Paper

Analytical characteristics of a commercial ICP orthogonal acceleration time-of-flight mass spectrometer (ICP-TOFMS)†

Ralph E. Sturgeon,*[a] Joseph W. H. Lam[a] and Andrew Saint[b]

[a]*Institute for National Measurement Standards, National Research Council of Canada, Ottawa, Canada K1A 0R9*
[b]*GBC Scientific Equipment Pty Ltd, 12 Monterey Road, Dandenong, Victoria 3175, Australia*

Received 18th January 2000, Accepted 21st March 2000
Published on the Web 28th April 2000

Analytical data illustrating the typical response characteristics of a commercial inductively coupled plasma orthogonal acceleration time-of-flight mass spectrometer (Optimass8000 ICP-*oa*-TOFMS, GBC Scientific Equipment Pty Ltd., Australia) are presented. With optimum instrument response tuned at mid-mass (^{103}Rh), limits of detection for a suite of elements representative of *m*/*z* 9–238 were estimated to be typically 1 ppt; background counts across the mass range averaged 0.5 Hz; sensitivity was 7 MHz per μg ml^{-1} (Rh); resolution (FWHM) ranged from 500 (^{7}Li) to 2200 (^{238}U); long-term drift over 700 min was 0.7% h^{-1}; abundance sensitivity was 2.8×10^{-6} (low mass side) and 7.4×10^{-5} (high mass side); mass bias ranged from 10% per u at ^{24}Mg to $<1\%$ per u at $m/z > 80$ and isotope ratio precision was demonstrated to be limited by counting statistics when the detector was operated in the pulse counting mode. Matrix effects, while relatively insignificant at 30 ppm NaCl and reaching 60–80% suppression of response at 3500 ppm, had no influence on the measured resolution, mass calibration or isotope ratio accuracy. The instrument faithfully recorded transient signals arising from flow injection sample introduction, from which isotope ratio information free of time skew could be generated.

Introduction

The recent introduction of ICP time-of-flight mass spectrometers (ICP-TOFMS) to the marketplace opens a number of practical advantages for the user, including: enhanced sample throughput and elemental coverage wherein a complete mass spectrum is generated from each ion-gating event; elimination of time (spectral) skew to permit reliable registration of multi-isotope signals from transient sample introduction devices such as laser ablation, flow injection and electrothermal vaporization; enhanced resolution; unlimited use of internal standards without performance compromises; and improved isotope ratio precision capability owing to the high correlation of the noise sources for all isotopes which occur with simultaneous sampling (extraction).

Unfortunately, the small number of laboratories currently operating ICP-TOFMS systems has not yet served to adequately characterize these performance parameters to an extent that permits potential users to comprehensively evaluate them for specific applications. Myers and Hieftje[1] first reported on the design and preliminary analytical characteristics of an ICP ion source coupled to a TOF mass analyzer. They concluded that orthogonally gated and accelerated (*oa*) sampling of the continuous supersonic expansion beam from the ICP provided for greater sensitivity, better duty cycle and higher resolution than was achievable with an axially accelerated (*aa*) configuration. The authors utilized post acceleration deflection fields (steering plates) in an attempt to maintain a perpendicular drift trajectory to the sampled length of the ion beam.[1,2] This has been shown to degrade the resolution of the *oa*-TOF relative to the use of a simple spontaneous drift trajectory wherein the axial velocity of the ion beam is conserved.[3–5] Additionally, significant mass bias effects, amounting to several percent per mass unit, have been reported with *oa* designs utilizing steering plates.[5] It has been shown that this shortcoming can be largely obviated by simply increasing the length of the sampled ion beam[6,7] such that the higher energy (higher mass) ions are transmitted to the detector from the trailing part of the ion packet while the lower energy ions are sampled from the leading part (closest to the detector in the beam direction). In this way a more uniform response over the mass range is obtained without the need for a large detector.

Recently, the analytical characteristics of a commercially available ICP-*aa*-TOFMS instrument (LECO Renaissance) were presented,[8,9] wherein the enhanced isotope ratio precision which accrues with TOF detection was highlighted. Unfortunately, apart from relative signal intensities (analog detection mode used) and precision data, Vanhaecke *et al.*[8] present little additional information with which to characterize the performance of the instrument from the perspective of the general user. Moreover, relatively high analyte solution concentrations were utilized (50–500 ng ml^{-1}) throughout the investigation. Tian *et al.*[9] provide a more exhaustive, quantitative evaluation of this instrument, presenting figures of merit in terms of accuracy, precision, resolution, detection limits, stability and isotope ratio precision. Emteborg *et al.*[10] further pursued evaluation of precision and mass bias for isotope ratio measurement in more detail using this TOFMS system, examining effects of detector voltage, integration window and time on accuracy and % RSD. Analog detection in combination with solution concentrations of 50–220 ng ml^{-1} were studied in an effort to reduce fundamental noise and to avoid both dead time corrections as well as contamination issues. For some elements at high signal intensities, RSDs of $<0.05\%$ could be obtained.

One of the more frequently used arguments in favour of TOF detection is the potential for elimination of the effects of drift and multiplicative (flicker) noise components in the source. Since all ions are sampled simultaneously from the ICP in each cycle of mass analysis, such effects can be compensated by ratioing techniques. Additionally, since the same detector is used (as opposed to multi-collector ratioing instruments), its

noise characteristics should be identical for signal ratioing. In reality, TOF detection provides near-simultaneous measurements, provided the mass dependence of the time required for the ions to pass through the ion optics between the skimmer and the flight tube is minimized.

It is the purpose of this study to present data characterizing the analytical performance of a commercially available ICP-orthogonal acceleration-TOFMS instrument (ICP-*oa*-TOFMS).

Experimental

Instrumentation

The Optimass8000 ICP-*oa*-TOFMS instrument (GBC Scientific Equipment Pty. Ltd., Australia), used throughout, has a 2×0.5 m flight tube fitted with a reflectron ion mirror, as outlined in the schematic presented in Fig. 1. The distance from the tip of the sampler orifice to the center of the *oa* extraction region is 33.5 cm. The instrument is equipped with an ion blanker located at the first space focus point downstream of the *oa* where ions of the same *m*/*z* are tightly bunched in space and time. A software selected voltage pulse applied to a series of strip electrodes produces a transient field designed to deflect a selected narrow range of *m*/*z* from the flight path. Multiple *m*/*z* regions are user selectable.

Samples were introduced using a concentric nebulizer (Glass Expansion Pty. Ltd., Camberwell, Victoria, Australia) coupled to a 70 ml thermostated (15 °C) cyclonic spray chamber (Glass Expansion). Liquid uptake rate was controlled by selection of the instrument peristaltic (12 roller) pump speed and arbitrarily set for approximately 0.5 ml min^{-1}. Ion detection is achieved by utilizing the discrete dynode electron multiplier (ETP, Ermington, NSW, Australia) in simultaneous pulse counting and analog signal collection modes. Instrument settings are summarized in Table 1. Data were stored in Microsoft Access files and subsequently exported to Microsoft Excel spreadsheets for manipulation.

Table 1 ICP-TOFMS operating conditions

ICP Source—	
Rf power (27.12 MHz)	1200 W
Plasma gas flow rate	10 l min^{-1}
Auxiliary gas flow rate	1.0 l min^{-1}
Nebulizer gas flow rate	0.680 l min^{-1}
Mass spectrometer—	
Ion optics	
Skimmer	−900 V
Skimmer base	0 V
Extraction	−900 V
Z1	−90 V
Y mean	−350 V
Y deflection	20 V
Z lens mean	−1200 V
Z lens deflection	−20 V
Lens body	−170 V
Pulse shaping	
Fill	−33 V
Fill bias	5.00 V
Fill grid	−8 V
Pushout plate	500 V
Pushout grid	−600 V
Spectral frequency	33 kHz
Reflectron	690 V
Detection	
Multiplier gain	2500 V
Ion threshold	2.0 mV
ADC offset	−2.0 mV
Integration window	Auto
Measurement mode	Pulse counting/analog

For the purpose of generation of "transient" signals, a simple flow injection manifold was constructed around a Model 5020 manually actuated 6-port low pressure sample injection valve (Rheodyne, Cotati, CA) fitted with a 35 µl

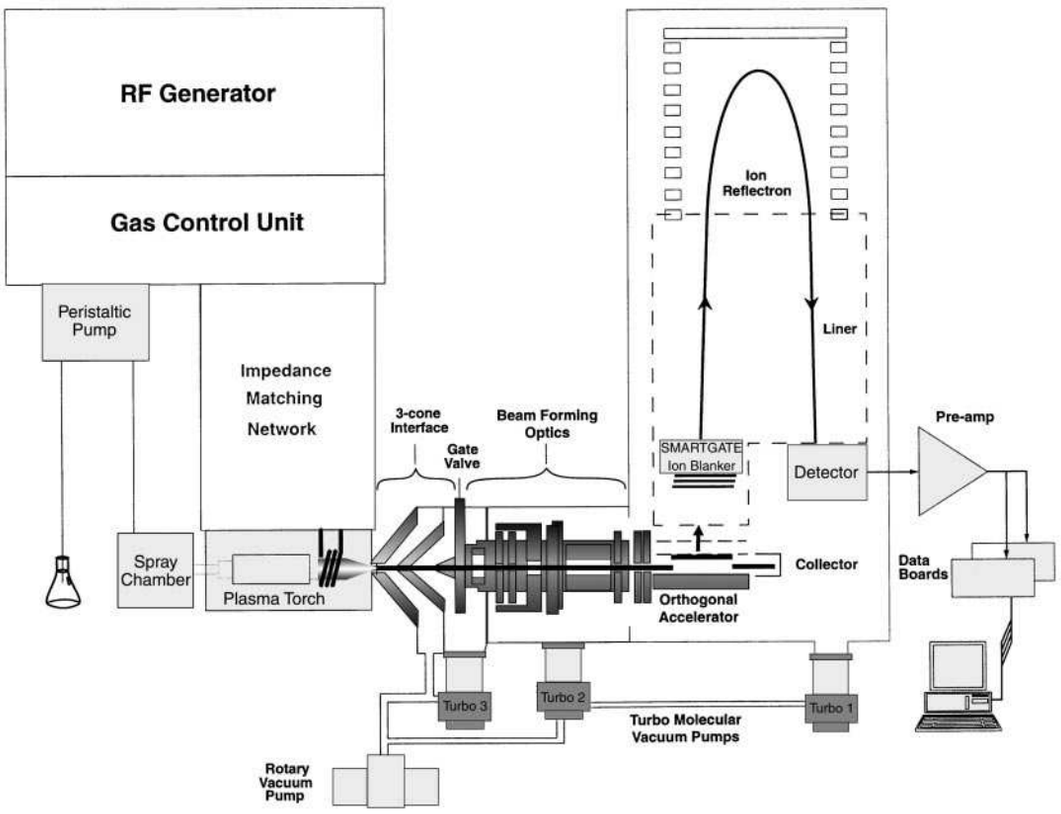

Fig. 1 Schematic outline of the GBC Optimass8000 ICP-*oa*-TOFMS instrument.

sample loop. Teflon tubing and flangeless fittings (UpChurch Scientific, Oak Harbor, WA) were used to connect the system to the nebulizer. A stand-alone Gilson Minipuls 3 peristaltic pump (Villiers Le Bel, France) propelled samples at a flow rate of approximately 0.3 ml min^{-1}. This accentuated the roller-induced pulsations from the pump and resulted in the FWHM of the analyte signals being of the order of 6 s with full baseline width of approximately 15 s. Data were collected for 20 s at intervals of 250 ms.

Reagents and standards

Distilled deionized water (DDW) was obtained from a NanoPure (Barnsted, UK) purification system. High purity HNO_3 and HCl were prepared in-house by sub-boiling distillation of the reagent grade feedstocks using a quartz still housed in a Class 10 fume cupboard. Stock solutions of the various elements were prepared by dissolution of the pure elements or their high-purity salts (Alfa Aesar, Ward Hill, MA) in acid followed by dilution with DDW and storage in pre-cleaned screw capped polypropylene bottles.

All test solutions were prepared in a Class 10 laboratory clean room. The instrument was located in a routine laboratory. A multi-element stock solution, containing Be, Co, Rh, La, Ce, Ho, Bi and U at concentrations of 10 μg ml^{-1}, was used to prepare a 1 ng ml^{-1} solution of the analytes containing 0.25% (v/v) HNO_3 which was used for the estimation of detection limits.

Isotope ratio measurements were undertaken using a series of multielement solutions at concentrations of 0.1, 1.0, 2.0, 10, 100 and 500 ng ml^{-1} containing Mg, Cu, Ag, Ce, Y, Pt, Tl and U. Ten replicate measurements were taken of each sample solution using integration times of 0.2, 1.0, 2.0, 5.0, 10.0, 20.0 and 50 s in order to assess the precision of isotope ratio measurement and the influence of counting statistics on the results. Mass bias was calculated as the difference between the measured and expected ratio.

The effect of matrix interference on response from analytes in a multielement solution containing 5 ng ml^{-1} U, Pb, Te, Cd, Ga, Ge, Yb and 10 ng ml^{-1} Be was examined. A series of these analyte solutions containing varying amounts of a seawater matrix was prepared by diluting NASS-5 Open Ocean Seawater reference material (NRCC, Ottawa) 10-, 100-, 1000-, 10000- and 100000-fold with 0.25% (v/v) HNO_3.

High and low mass abundance sensitivity was estimated from measurements of signal intensities from a solution containing 50 pg ml^{-1} Sr, 500 pg ml^{-1} Zr and 1 μg ml^{-1} Y. A 1 s acquisition (integration) time was suitable for this purpose.

Multielement solutions containing Ag, Ce, Cu, Ir, Mg, Pt, Tl and Yb at concentrations of 1, 10, 100 and 1000 ng ml^{-1} were prepared for introduction with the sampling loop to generate transient signal data.

Procedures

Instrument tuning was optimized at mid-mass range and based on peak count response from Rh. Conditions, summarized in Table 1, achieved a sensitivity of 7 MHz per μg ml^{-1} (mass integrated peak) and a resolution (FWHM) of 1460. Mass calibration was achieved using responses from $^{23.99}Mg$, $^{102.91}Rh$ and $^{207.98}Pb$.

Detection limits were calculated from the measured sensitivities (using a 1 ng ml^{-1} solution) and estimated standard deviations of the blank consisting of 0.25% (v/v) HNO_3. For this purpose, a signal acquisition time of 10 s was set and 10 replicate measurements were acquired. Instrument background (Hz) across the mass range was estimated from 10 replicate 10 s data acquisitions obtained during nebulization of the blank solution; measurements at *m/z* values of known potential contaminants (Na, Mg, *etc.*) were avoided.

Long-term stability of the instrument was examined by running a multielement solution containing 2 ng ml^{-1} of the analytes used for isotope ratio measurements. Data were collected overnight at a frequency of one sample per min for 700 min using a signal acquisition time of 10 s.

Isotope ratio precision was evaluated from a series of measurements on a multielement solution for which the integration (acquisition) time was varied between 0.2 and 50 s and whose concentrations ranged from 0.1 to 500 ng ml^{-1}. In all cases, 10 replicate 10 s measurements were taken, from which the experimental % RSD of the ratio of two or more isotopes of each element was compared with the theoretical count limited statistic.

Matrix effects arising from the presence of increased concentrations of NaCl (along with some Ca and Mg arising from the seawater) were evaluated by normalising the response from each sample to that obtained from a matrix-free solution of the analytes. Eight replicate 5 s integrations were made of each solution.

"Transient" signals were generated by manual introduction of discrete 35 μl volumes of sample using a flow injection system interfaced to the instrument. Isotope ratio information was evaluated with this mode of sample introduction, as was calibration stability and linearity of response.

Results and discussion

This study was undertaken in an effort to characterize this technique from a typical user's perspective; to provide unbiased performance information with ICP-*oa*-TOFMS that may serve to guide interested users in assessing its potential for specific applications and to highlight the current shortcomings of this approach to detection for ICP-MS. It is to be noted that all experiments were recorded under instrument conditions which were first optimized with respect to both peak height sensitivity and peak shape (resolution) for response from ^{103}Rh. Ion blanking (application of a transverse voltage deflection pulse to prevent unwanted ions from reaching the detector) was activated to cover the *m/z* range 10–22, as well as 28–42 and 75–85, thereby minimizing response from $^{14}N^+$, $^{16}O^+$, $^{17}OH^+$, $^{18}H_2O^+$, $^{28}N_2^+$, $^{30}NO^+$, $^{32}O_2^+$, $^{40}Ar^+$, $^{41}ArH^+$ and $^{80}Ar_2^+$ whenever possible during measurements.

An important advantage of *oa*-TOFMS is the minimization of the spread of initial ion velocities in the beam drift direction (average velocity is zero) which serves to increase the achievable resolving power. Resolution, defined as the full width at half maximum intensity (FWHM), ranges from approximately 500 for ^{6}Li to at least 2200 for ^{238}U under compromise tuning conditions (although a resolution of 2400 can be selectively achieved for ^{103}Rh). Resolving power decreases towards low mass due to the constant contribution of the detector pulse width and jitter of the timing electronics.[11] In all cases, tuning was achieved by altering the voltages applied to all tuning elements with the exception of the reflectron, which was maintained at 690 V throughout. Unfortunately, the practical advantages of such resolution are minimal for the user. Potential cases, where advantage may be taken of this aspect of instrument performance relative to a standard quadrupole machine, relate to the elimination of isobaric interference from NOH on the measurement of ^{31}P, wherein a practical resolution of 967 is required and attainable, and that of ^{28}Si to be discerned from $^{14}N_2$ wherein a resolution of 958 is required.

Limit of detection and background

Fig. 2 illustrates typical LODs and background count obtained for a number of elements representative of the mass range of interest. In all cases, the integration window (time window or mass width window), although operator selectable, was used

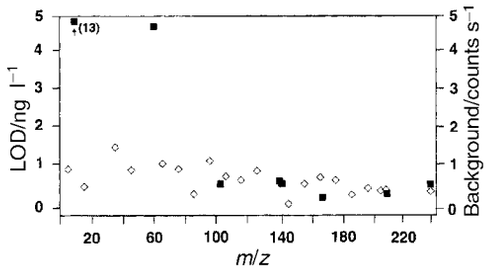

Fig. 2 Limit of detection and background for compromise tuning at ^{103}Rh: ■ LOD, ◇ background.

with default parameters specified by the manufacturer which varied from 0.108 amu at Be to 1.000 amu at U. Detection limits were based on a $3s_b$ criterion wherein the standard deviation of 10 replicate 10 s integrations of 0.25% (v/v) HNO_3 in DDW were acquired followed by a measure of the sensitivity of each isotope of interest using a 1.0 ng ml^{-1} multielement standard solution in 0.25% (v/v) HNO_3. In general, LODs are comparable to those reported for many quadrupole-based instruments operating with much higher sensitivity[12] and are approximately an order of magnitude lower than those recently reported by Tian *et al.*[9] using an ICP-*aa*-TOFMS instrument. Relatively low background counts are achieved across the mass range. The absence of a direct line-of-sight geometry between the sampled beam and the detector, coupled with efficient removal of neutrals from the drift region, minimize scatter and secondary ion generation, thereby reducing this parameter. It should be noted that, as the instrument was optimized for ^{103}Rh, LODs could likely be improved for Be and Co if tuning was undertaken in the low mass range. It is possible to achieve a 6-fold increase in sensitivity for ^{24}Mg by retuning the instrument at this *m*/*z*. Under compromise conditions, the sensitivity rises rapidly from 0.4 MHz per μg ml^{-1} at *m*/*z* 9 to 3.5 MHz at *m*/*z* 60, reaching 7 MHz per μg ml^{-1} at *m*/*z* 103, whereupon it remains approximately constant to *m*/*z* 209.

Long- and short-term stability

Short-term stability (20 measurements taken over a 20 min interval) was characterized by an approximately 1% RSD. A series of measurements on a multielement solution containing 2 ng ml^{-1} Mg, Cu, Ag, Ce, Y, Pt, Tl and U was run unattended overnight and the resulting long-term drift in the data evaluated. Fig. 3a illustrates results obtained for cerium, silver, copper and magnesium. Data collection started 1 h after the plasma was ignited, the instrument tuned and the method set up. Over the course of 700 min, during which time a single 10 s integration was made at 1 min intervals, signal intensity drifted an average of 0.7% per h downward for Ag, Cu and Mg and upward by 0.2% per h for Ce. Silver presents the worst case scenario, with the majority of the drift occuring rather quickly during the final 3.5 h. Fig. 3b illustrates the long-term stability of the ^{107}Ag/^{109}Ag ratio. Following an initial 20 min period of data collection, ratio stability becomes quite good; as expected, ratioing eliminates the effect of drift on the response and a second isotope of an element serves as an ideal internal standard. Without applying any mass bias correction factor to the data, the average isotope ratio from all 700 data points for Ag is 1.078 ± 0.007 (true value: 1.0764). The average of the last 10 data points (final 10 min of signal acquisition) is 1.076 ± 0.007, demonstrating that instabilities in residual factors which may lead to changes in the ratio with time, such as mass bias and mass calibration drift, are negligible over a period of nearly 12 h of continuous operation. It is interesting to note, however, that instability over a much shorter time scale, of the order of a few minutes, occurs as a result of intermittent noise unequally influencing the isotopes of interest. This gives rise to the spiked appearance of the ratio data

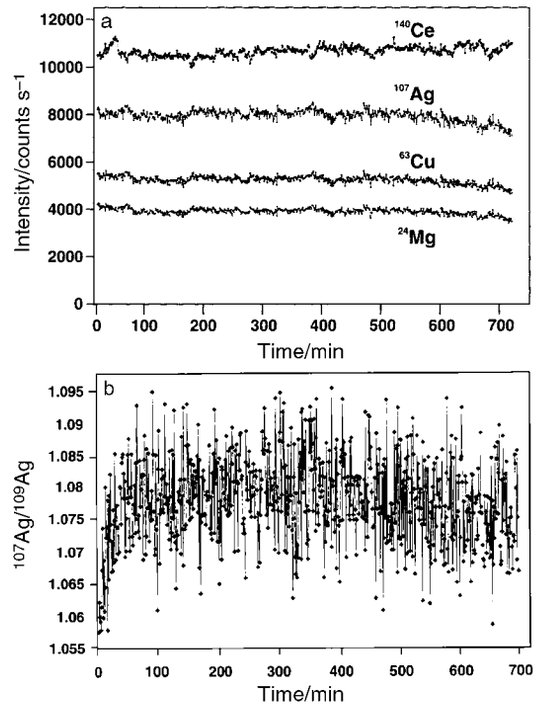

Fig. 3 Long-term signal stability for (a) ^{140}Ce, ^{107}Ag, ^{63}Cu and ^{24}Mg using pulse counting with a 2 ng ml^{-1} solution and 10 s integration every minute; and (b) long-term stability of ^{107}Ag/^{109}Ag ratio under above conditions.

evident in Fig. 3b, similar to that reported by Begley and Sharp[13] who identified the source of such fluctuations as instabilities in the mass calibration and mass bias of their instrument. Mass calibration was observed to be extremely stable; drift in the position of the mass peak of any given isotope was never more than 0.02 amu over a continuous 7 d period of operation. However, short-term fluctuations in the ion optic voltages may give rise to altered isotope transmission efficiencies creating fluctuations in mass bias; this aspect of instrument performance requires further study. Data presented in Fig. 3b for silver are typical of that for all other elements investigated.

Abundance sensitivity

Abundance sensitivity for quadrupole instruments is typically $<1\times10^{-6}$ on the low mass side and $<1\times10^{-7}$ on the high mass side.[12] Using ^{89}Y as the "perturbing" isotope, abundance sensitivity was evaluated at ^{88}Sr and ^{90}Zr. An intense peak from ^{89}Y (2.2 MHz) was generated by the introduction of a solution containing 1 μg ml^{-1} Y. Fig. 4 illustrates the signal arising from concurrent introduction of a 50 pg ml^{-1} solution of Sr, permitting calculation of the contribution of the leading edge of the ^{89}Y peak under the ^{88}Sr peak (equivalent to the introduction of a solution containing 4 pg ml^{-1} Sr) and a measure of the abundance sensitivity to be 2.8×10^{-6} at a resolution of 1450. A similar, direct measurement on the high mass side using a 1 μg ml^{-1} solution of Y containing 500 pg ml^{-1} Zr was not possible due to ringing in the pulse counting detector circuit. This problem was minimized by application of the ion blanking system to attenuate the response from Y. Under these conditions, a clear tailing in the signal is evident on the high mass side of ^{89}Y, yielding an elevated background under the ^{90}Zr peak, estimated to be equivalent to 140 pg ml^{-1} ^{90}Zr and yielding an abundance sensitivity of 7.4×10^{-5}. It may be argued that the use of the ion blanker to attenuate the unwanted ($m-1$) signal intensity does not permit calculation of a standard abundance sensitivity that may be used for comparison with a quadrupole machine.

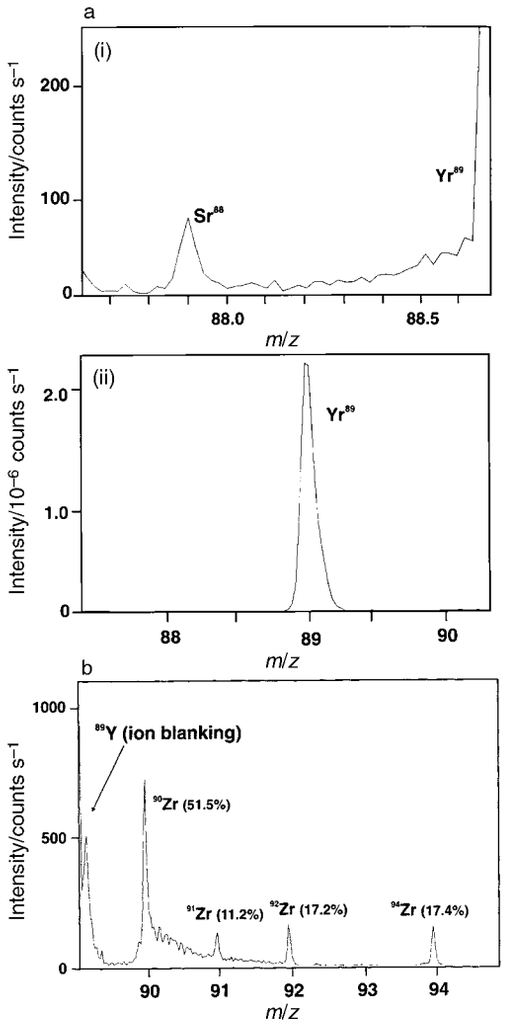

Fig. 4 (a) Low mass abundance sensitivity as exemplified by detection of 50 pg ml^{-1} ^{88}Sr (FWHM resolution = 1457) in the presence of 1 μg ml^{-1} ^{89}Y: (i) pulse counting, abundance sensitivity = 2.8×10^{-6}; (ii) analog detection. (b) High mass abundance sensitivity as exemplified by detection of 500 pg ml^{-1} ^{90}Zr in the presence of 1 μg ml^{-1} ^{89}Y: pulse counting, abundance sensitivity = 7.4×10^{-5} (note: blanker system used to attenuate response from ^{89}Y for high mass experiment).

Clearly, the ion blanking system can be used to such advantage. An alternative means of interpreting the data under such conditions may lie with the calculation of an equivalent concentration at the $(m+1)$ mass which, for ^{90}Zr is, as stated above, 140 pg ml^{-1}. This results in a calculated high-mass abundance sensitivity of 1.4×10^{-4} for this particular situation. A quick survey of relative peak intensities generated for the four isotopes of Zr in one spectral scan, displayed in Fig. 4b, reveals that they follow the expected abundance pattern, *i.e.*, 5 : 1 : 1.5 : 1.5 for Zr 90 : 91 : 92 : 94, with little perturbation arising from the use of the ion blanker at $m/z = 89$.

Despite the fact that abundance sensitivity is inferior to that obtained with a quadrupole based system,[12] the full spectrum capability of the TOFMS is advantageous in that it quickly permits "on-line" calculation of any correction required as a consequence of finite abundance sensitivity for any element pairs.

Isotope ratio precision

If the majority of non-random flicker noise is removed by isotope ratioing and signal averaging, the counting statistic would likely be precision limiting, as dictated by Poisson statistics. Any remaining fluctuation in the ratio then likely comes from mass bias and mass calibration instabilities.[13] With TOFMS, each spectrum acquired represents signals from ions extracted from the plasma during the same time interval, formed from identical plasma and sample introduction events.

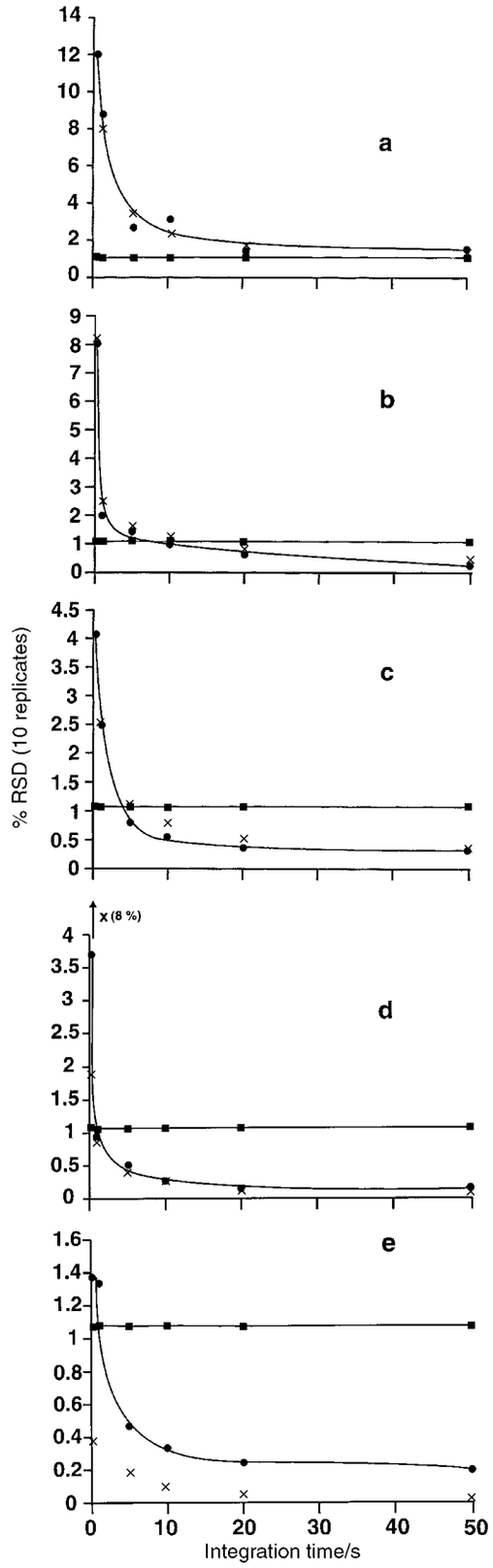

Fig. 5 Effect of signal acquisition time on isotope ratio precision for ^{107}Ag/^{109}Ag: (a) 0.1 ng ml^{-1}; (b) 1.0 ng ml^{-1}; (c) 2 ng ml^{-1}; (d) 10 ng ml^{-1}; (e) 500 ng ml^{-1}. Data reflects average of 10 replicates. ●, Experimental precision; ×, calculated statistical limit of expected ratio precision based on total counts for each isotope; ■, calculated ratio (not corrected for mass bias or background).

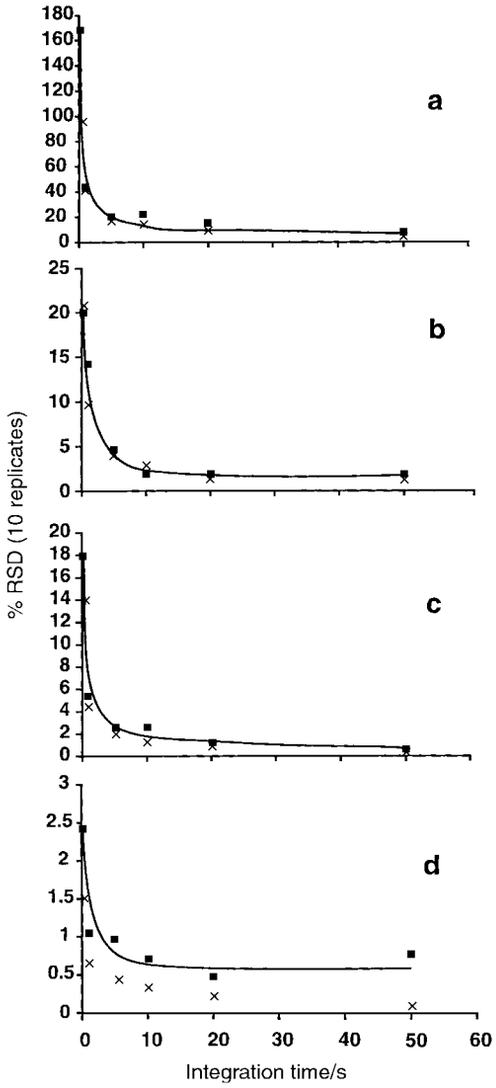

Fig. 6 Effect of signal acquisition time on isotope ratio precision for $^{235}U/^{238}U$: (a) 0.1 ng ml^{-1}; (b) 2.0 ng ml^{-1}; (c) 10 ng ml^{-1}; (d) 500 ng ml^{-1}. Data reflects average of 10 replicates. ■, experimental precision; ×, calculated statistical limit of expected ratio precision based on total counts for each isotope.

As a consequence, TOFMS should be able to achieve excellent precision for any number of elemental isotope pairs in a single acquisition, subject to statistical limits wherein the acquisition time must allow sufficient ions to be detected (*e.g.*, ten 10 s integrations on a 1 ng ml^{-1} solution of an element having an isotope ratio of 1, to result in a 0.1% RSD[14,15]).

Figs. 5 and 6 illustrate ratio data obtained for Ag and U, these elements presenting two extreme examples for isotope ratio determination. Whereas the natural abundance of the silver isotopes is near unity and ideal for the purposes of demonstrating counting statistic limitations at any analyte concentration, the 235/238 ratio for U is 10^{-2}, which may require a combination of pulse counting and analog detection if the analyte solution concentration is higher than 5 ng ml^{-1}.

At concentrations of 0.1, 1.0, 2 and 10 ng ml^{-1}, pulse counting detection of both the 107 and 109 isotopes of Ag occurs. Beyond 10 ng ml^{-1}, the analog detection circuit is operative for both isotopes (cross-over is currently set at 25 kHz; a 7.5 ns detector dead time was accounted for in the software). It is evident from Fig. 5 that the % RSD of the isotope ratio can, in general, be modelled quite well with a shot noise limited statistic and, for any given concentration, the isotope ratio precision generally improves as the [acquisition time]$^{1/2}$ or as the [analyte concentration]$^{1/2}$ for a given acquisition time. At a concentration of 500 ng ml^{-1}, there appears to be instabilities in the analog circuit, as the statistical limit of the precision is not achieved under any conditions due to the presence of some uncharacterized noise source. Accuracy of the $^{107}Ag/^{109}Ag$ ratio is maintained in all cases with isotope ratios (not corrected for mass bias nor background) calculated from the average of the 6 integration periods (0.2, 1,5, 10, 20 and 50 s) for concentrations of 0.1, 1.0, 2.0, 10.0 and 500 ng ml^{-1} being 1.06 ± 0.02, 1.076 ± 0.003, 1.075 ± 0.004, 1.071 ± 0.006 and 1.076 ± 0.003, respectively (accepted value 1.0764[16]).

For uranium, both isotopes can be measured using the pulse counting mode for concentrations of 0.1 and 2.0 ng ml^{-1}. In such case, the %RSD for the measured ratio is tracked quite well by the Poisson statistic. At a concentration of 10 ng ml^{-1}, ^{235}U is measured using the pulse counting mode and ^{238}U is measured using the analog circuit. The consequence is that not only is there degradation in the precision with which the ratio is measured, but the ratio is inaccurate, probably a consequence of inappropriate calibration of the cross-over from the pulse counter to analog detector modes. Finally, at 500 ng ml^{-1}, both isotopes exhibit sufficient intensities to permit measurements in the analog mode only. It is evident from the data in Fig. 6 that isotope ratio precision in this mode is better than that achieved in the mixed detector mode, but that inaccuracy is again present, *i.e.*, 0.0051 ± 0.0001 *vs* 0.0073 ± 0.0001 at 2 ng ml^{-1}. This may arise as a result of an incorrect ADC offset voltage for this detector (Table 1) which would compromise the intensities of the ^{235}U isotope significantly more than that of the ^{238}U isotope.

Table 2 summarizes the isotope ratio precisions obtained using different acquisition times for 1.0 and 10 ng ml^{-1} multi-element solutions, respectively. In general, it is evident that precision improves with increase in either integration (acquisition) time or analyte concentration, typically following a square root dependence on either parameter. Isotope ratio precisions of the order of 1% RSD can be achieved with a 1 ng ml^{-1} solution concentration using modest 10 s acquisition times, irrespective of the number of ratio pairs considered. Precisions can be improved to 0.2% RSD using a 10 ng ml^{-1} analyte solution and 50 s acquisition time. This level of precision is comparable to that currently available with most quadrupole-based instruments using similar integration times[12,15] and is similar to that recently reported by Tian *et al.*[9] for their *aa*-TOF-MS instrument, although the latter was achieved using analog detection with solution concentrations an order of magnitude higher than employed in this study. It is noteworthy that the precision of some isotope pairs (Ag, Ce and Tl) actually degraded when acquisition times of 50 s were used. The reason for this is not clear at this time; detector saturation is not an issue and pulse counting was utilized for the 1.0 ng ml^{-1} solution. This is consistent with observations made in connection with the data reported in Fig. 3b. Similar reversals in precision have also been noted with data obtained using an ICP-*aa*-TOFMS instrument.[8]

Mass bias

Mass bias is the deviation of the measured isotope ratio from the actual value, which arises because the sensitivity of the instrument varies with mass due to differences in ion transmission efficiency. Utilizing data obtained in the above experiment permitted a mass bias response curve to be generated, which is shown in Fig. 7. In the case of uranium, a natural abundance was assumed to be present in the laboratory prepared sample solution. The mass bias per mass unit is typical of that reported for quadrupole- and sector-based instruments[15] and at mid-mass (Ag) amounts to 0.12%. By retuning the system (normally optimized for ^{103}Rh) at the

Table 2 Isotope ratio precision for varying acquisition times (%RSD, $n=10$)

Time/s	$^{25}Mg/^{24}Mg$	$^{65}Cu/^{63}Cu$	$^{107}Ag/^{109}Ag$	$^{140}Ce/^{142}Ce$	$^{171}Yb/^{173}Yb$	$^{195}Pt/^{194}Pt$	$^{205}Tl/^{203}Tl$	$^{235}U/^{238}U$
1.0 ng ml^{-1}								
0.2	1.8	13	8.1	6.4	6.7	5.5	5.2	21
1.0	1.1	5.4	2.0	3.3	2.8	3.2	2.4	20
5.0	0.47	1.5	1.5	2.6	1.6	2.4	0.86	8.1
10	0.37	1.5	0.95	1.1	1.1	1.3	0.88	4.0
20	0.28	1.0	0.61	0.47	0.91	0.81	0.35	4.0
50	0.11	0.72	0.23	0.54	0.60	0.44	0.44	2.6
10 ng ml^{-1}								
0.2	1.2	5.2	3.7	3.7	3.9	3.4	5.1	18
1.0	0.32	1.2	0.96	1.5	1.2	1.4	1.1	5.4
5.0	0.13	0.79	0.52	1.2	0.68	0.53	0.57	2.6
10	0.11	0.31	0.26	1.0	0.62	0.42	0.46	2.6
20	0.06	0.39	0.15	0.78	0.28	0.37	0.34	1.2
50	0.04	0.26	0.17	0.28	0.16	0.19	0.25	0.55

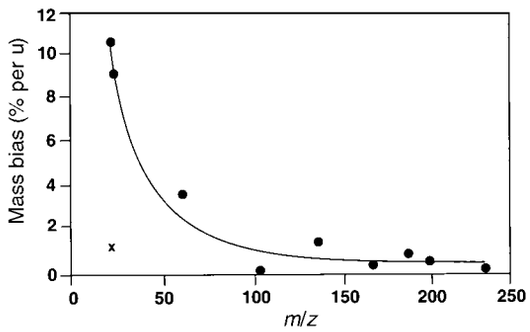

Fig. 7 Mass bias characteristics of an *oa*-TOF instrument: ●, calculated mass bias for compromise tuning at ^{103}Rh; ×, mass bias with instrument tuned at *m/z* 24.

low mass end, based on response from Mg, the mass bias at *m/z* 24 could be reduced from 11% to as little as 1%. It has been suggested[8] that mass bias in a ICP-*oa*-TOFMS system is likely much higher than that in an *aa*-TOF system because of the residual perpendicular (to the drift direction) velocity component of the sampled ion beam. Even in the absence of steering plates to alter beam trajectory, no deleterious effects are evident in the mass bias performance of this instrument, which is comparable to that reported by Tian *et al.*[9] for their *aa*-TOF instrument.

The effects of matrix concomitants on mass bias are discussed below.

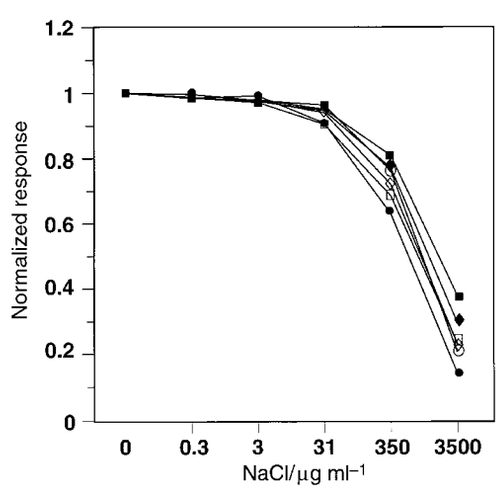

Fig. 8 Influence of NaCl matrix on the normalized response from U, Pb, Te, Ga, Y (5 ng ml^{-1}) and Be (10 ng ml^{-1}). Eight 5 s integrations were averaged for each element: ■ ^{235}U; ◇ ^{69}Ga; ○ ^{9}Be; □ ^{208}Pb; ◆ ^{174}Yb; ● ^{125}Te.

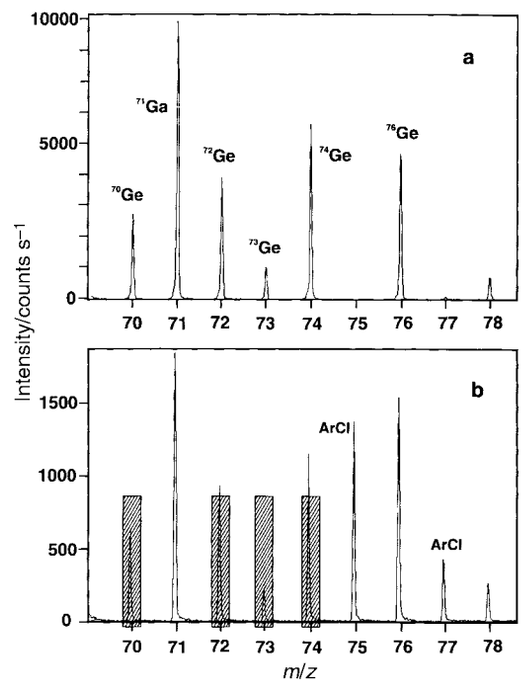

Fig. 9 Mass spectral scans centered on Ge for solutions containing 5 ng ml^{-1} Ge and (a) 0.35 μg ml^{-1} NaCl and (b) 3500 μg ml^{-1} NaCl. Note suppression of response due to NaCl and appearance of ArCl. Resolution (FWHM) at *m/z* 76 = 1497.

Matrix effects

The influence of increasing concentrations of NaCl on response from a number of elements selected to span the entire mass range is summarized in Fig. 8 (not shown are responses from Cd and Ge in an effort to simplify the display). The effects noted are due to non-spectral interferences, except for a perturbation of the ^{125}Te isotope intensity due to polyatomic isobaric $^{88}Sr^{37}Cl^{+}$ ion present in the diluted seawater matrix. No attempt was made to minimize the matrix effect by retuning the instrument or changing the nebulizer gas flow rate. In general, the severity of the effect follows in the order Te > Be > Ga > Pb > Yb > U, with signals from U being least perturbed. No general trend can be discerned; the above order is neither that predicted from a classical space charge model of interference nor that attributed to ionization of the sodium producing an easily ionized element interference. The effects noted may be a convolution of these and other unappreciated factors. Figs. 9 and 10 show mass spectral scans centered on Ge and Pb, respectively, for signals generated from solutions containing disparate amounts of matrix. It is clear that increasing the concentration of NaCl by 10,000-fold has no

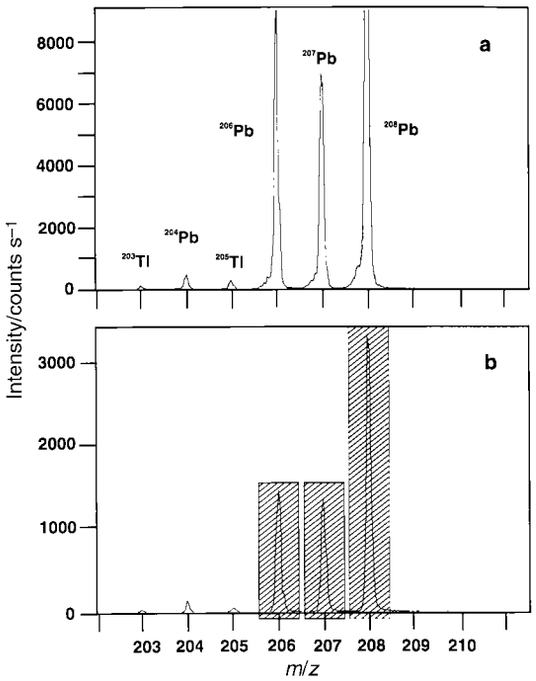

Fig. 10 Mass spectral scans centered on Pb for solutions containing 5 ng ml^{-1} Pb and (a) 0.35 µg ml^{-1} NaCl and (b) 3500 µg ml^{-1} NaCl. Resolution (FWHM) at *m/z* 208 = 2231.

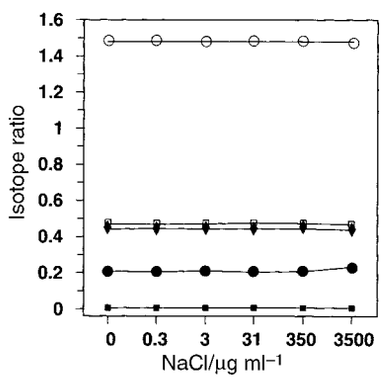

Fig. 11 Effect of increasing concentration of NaCl on isotope ratios obtained from solutions containing 5 ng ml^{-1} Ge, Pb, Yb, Te, U and 10 ng ml^{-1} Be. Eight 5 s integrations were averaged for each element: ○ ^{69}Ge/^{71}Ge; □ ^{206}Pb/^{208}Pb; ◆ ^{171}Yb/^{174}Yb; ● ^{125}Te/^{128}Te; ■ ^{235}U/^{238}U.

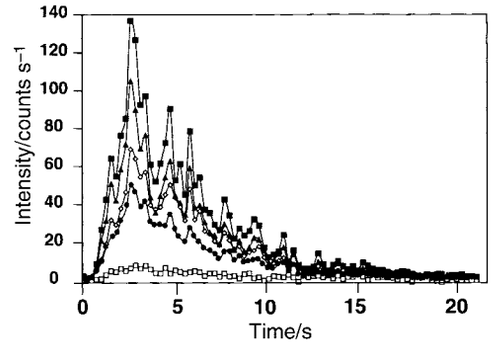

Fig. 12 Transient signal profiles for the FI introduction of a 35 µl loop of a solution containing 10 ng ml^{-1} of the analytes of interest. Data collected at intervals of 250 ms over a 20 s measurement period.

significant influence on either the mass calibration of the instrument (within the time frame of the experiments) or the resolution such as to alter the integration window.

One means to minimize matrix interferences is the use of internal standards to compensate for changes in response. If the matrix suppression effect on ion transmission efficiency is not uniform, however, compensation by such means will be ineffective. Clearly, the ideal internal standard is another isotope of the same element. The effect of increasing the matrix on the isotope ratio is illustrated in Fig. 11 for several elements. With the exception of the ^{125}Te/^{128}Te pair (due to isobaric interference from increasing amounts of ^{88}Sr^{37}Cl), the influence of the NaCl is completely obviated by ratioing. The average ratios (n = 6, uncorrected for background or mass bias) are: 1.479 ± 0.27% for ^{69}Ge/^{71}Ge; 0.466 ± 1.3% for ^{206}Pb/^{208}Pb; 0.442 ± 0.50% for ^{171}Yb/^{174}Yb; 0.207 ± 1.2% for ^{125}Te/^{128}Te; and 0.00713 ± 1.3% for ^{235}U/^{238}U.

Transient signals

The isotope ratio precision which accrues even for short acquisition times suggests good performance by the instrument for the measurement of transient signal information. Fig. 12 illustrates data obtained for several representative isotopes generated during the introduction of a 35 µl volume of a 10 ng ml^{-1} concentration of a multielement standard. Integrated full mass spectra were obtained every 250 ms over a total measurement period of 20 s (80 points). The average duration of the event, expressed as the FWHM of the "transient", is approximately 6 s. The sample introduction rate was sufficiently low that the pulsations of the peristaltic pump rollers can be clearly discerned. With an uptake rate of the DDW

Table 3 Isotope ratio and precision for transient sample introduction; 35 µl volume sample loop

	Concentration/ng ml^{-1}			
	1	10	100	1000
^{25}Mg counts^{a}	18	98	942	9553
^{25}Mg/^{26}Mg^{b}	−0.7 ± 4.2	0.89 ± 0.28	0.87 ± 0.05	0.87 ± 0.02
% RSD$_{exp}$	575	31	5.3	2.8
% RSD$_{theor}$^{c}	36	14	4.4	1.4
^{65}Cu counts	33	342	3350	24094
^{63}Cu/^{65}Cu	2.5 ± 0.9	2.2 ± 0.2	2.11 ± 0.08	1.45 ± 0.41
% RSD$_{exp}$	35	7.7	3.6	28
% RSD$_{theor}$	21	6.5	2.1	—
^{107}Ag counts	88	1081	7829	31084
^{107}Ag/^{109}Ag	1.12 ± 0.27	1.09 ± 0.08	1.10 ± 0.03	1.10 ± 0.04
% RSD$_{exp}$	24	7.3	2.7	3.2
% RSD$_{theor}$	15	4.4	1.6	0.8

^{a}Total counts between 1.5 and 10 s of transient. ^{b}Average ratio calculated from (n = 34) 250 ms signal integrations across the transient (not corrected for background or mass bias). ^{c}Statistical limit of precision based on total signal counts, all data obtained with pulse counting detection.

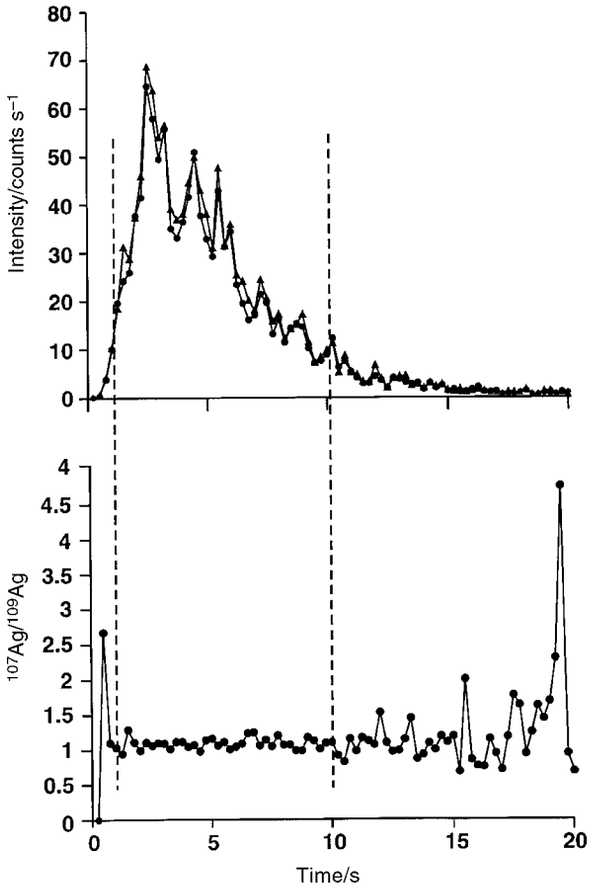

Fig. 13 Signal transient for FI introduction of a 35 µl volume of a solution containing 10 ng ml^{-1} ^{107}Ag and ^{109}Ag and the corresponding isotope ratio. Cursors delineate the region over which signal intensities are sufficient (for silver) for reliable calculation of ratios: ▲ ^{107}Ag; ● ^{109}Ag.

carrier solution of 0.3 ml min^{-1}, the introduction of a 35 µl volume of analyte solution should take about 7 s; the full-width of the signals (approximately 15 s) is a consequence of the dispersion of the sample in the carrier line (approximately 40 cm long) as well as the wash-in and wash-out characteristics of the spray chamber.

Calibration curves were constructed for each isotope based on a measure of the total integrated counts under the corresponding transient peaks. Linearity over the concentration range used (1–1000 ng ml^{-1}) was achieved with pulse counting detection provided the measured intensity did not result in detector saturation. Examples of such data are summarized in Table 3, wherein it is evident that the signal for the less abundant ^{25}Mg isotope provides for linear response over the full concentration range examined (the consistency of the ^{25}Mg/^{26}Mg ratio also points to linearity in the ^{26}Mg response) but those for Cu and Ag indicate non-linearities at concentrations exceeding 100 and 10 ng ml^{-1}, respectively.

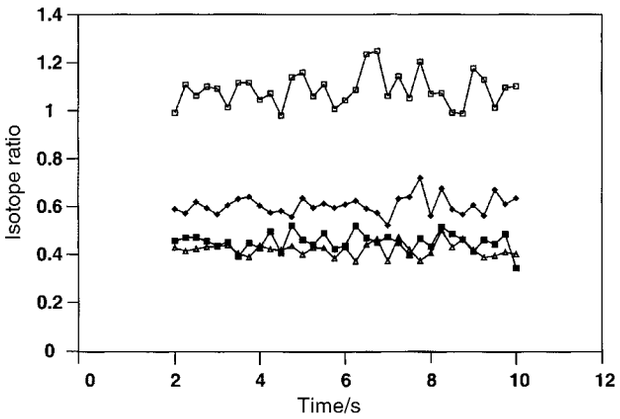

Fig. 14 Isotope ratios (uncorrected for background or mass bias) calculated across the central portion of the signal profile arising from the FI introduction of a 35 µl volume of a 10 ng ml^{-1} solution of analytes: □ ^{107}Ag/^{109}Ag (1.09±0.08); ◆ ^{191}Ir/^{193}Ir (0.60±0.02); ■ ^{65}Cu/^{63}Cu (0.45±0.35) and △ ^{203}Tl/^{205}Tl (0.42±0.01).

Fig. 13 shows data for the ^{107}Ag and ^{109}Ag intensities as well as their corresponding ratio as a function of time during the transient. Although a TOF mass analyser does not detect ions of different *m*/*z* simultaneously, all ions within a given extraction volume are pulsed into the drift tube at the same time. The good temporal correlation of the intensities for the two isotopes is evident and it is seen that their corresponding ratio remains invariant in time provided sufficient numbers of ions are detected to permit a reliable measurement; outside the central portion of the signal the intensities over the leading and falling edges beyond the 2 and 10 s cursor limits are too small to generate sensible ratio data. This is further illustrated for several isotope pairs by the data in Fig. 14, encompassing the time period between 2 and 10 s wherein a reasonable signal-to-noise ratio characterizing the transient can be found for the introduction of a 10 ng ml^{-1} solution. Despite the small signal intensities, averaged isotope ratios (calculated at 250 ms intervals, $n=33$) across the selected portion of the transient have associated precisions on the order of 2% (Tl)–8% (Cu) RSD.

The influence of the analyte concentration on the count limited precision expected for several representative isotope ratio pairs is summarized in Table 3. The selection was based on elements for which pulse counting detection was used for both isotopes of interest over the majority of the full concentration range (1–1000 ng ml^{-1}). As discussed earlier, the response is linear for Mg over the full concentration range, whereas those for Cu and Ag are non-linear as the concentration approaches 100 ng ml^{-1} and the signals are clearly saturated at 1000 ng ml^{-1}. Under conditions for which the detector is not saturated for either isotope, their ratio remains relatively invariant as the analyte concentration increases, but the precision of their determination is enhanced, the latter tracking the precision predicted by a counting statistic limit reasonably well. Clearly, the methodology is thus well-suited to the application of isotope dilution or use of other internal standards for calibration purposes.

Conclusions

The full versatility of the Optimass8000 ICP-*oa*-TOFMS has clearly not been exploited in the present study. Nevertheless, sufficient performance information has been generated to permit several conclusions to be discerned. The instrument is well-suited to the acquisition of transient signal information and, although currently limited to an 8 ms temporal resolution for full mass scan events, this is more than sufficient for applications with FI, ETV and various chromatographic sources of analyte introduction. Mass discrimination and low mass abundance sensitivity are comparable to those reported for quadrupole-based instruments but high mass abundance sensitivity is quite inferior. The problem at present appears to be related to detector ringing. Sensitivity is inferior to current quadrupole-based instruments, but the low background count rate still permits low pg ml^{-1} detection limits to be achieved. This sensitivity limitation ultimately restricts the precision of isotope ratio measurements at low concentrations and short measurement times, since counting statistics have been shown to govern the RSD of the measured ratios when pulse counting is employed. Limited sensitivity may also place restrictions on transient signal acquisition parameters in that compromises

must be made in setting the time resolution of events so as to ensure realistic count rates during each ion gating event. As an example, to achieve a 10% precision of measurement, a minimum of 100 counts must be accumulated for any analyte, integrated over the course of the event. If the time resolution required is 100 ms, the solution concentration of the analyte currently needs to be >0.1 ng ml^{-1}. For faster events, the concentration must be increased to maintain the same % RSD. It is evident that the introduction of effluents from gas chromatographic sources eases this restriction considerably due to this enhanced efficiency of sample introduction. These advantages have recently been exploited by Leach *et al.*[17]

It remains to investigate residual sources of noise which appear to limit ratio precisions achievable with long integration periods, as well as to examine more closely factors governing the long-term stability of these ratios. Analog detection with this instrument currently does not serve to enhance isotope ratio precision to the levels expected when using high analyte concentrations.

Acknowledgement

The authors thank Lindsay Moore and Peter Sanders (GBC Scientific Equipment Pty Ltd.) for their support of, and numerous suggestions for, this study.

References

1 D. P. Myers and G. M. Hieftje, *Microchem. J.*, 1993, **48**, 259.
2 D. P. Myers, G. Li, P. Yang and G. M. Hieftje, *J. Am. Soc. Mass Spectrom.*, 1994, **5**, 1008.
3 M. Guilhaus, *J. Am. Soc. Mass Spectrom.*, 1994, **5**, 588.
4 M. Guilhaus, V. Mlynski and D. Selby, *Rapid Commun. Mass Spectrom.*, 1997, **11**, 951.
5 J. Coles and M. Guilhaus, *Trends Anal. Chem.*, 1993, **12**, 203.
6 D. Bandura and R. Peile Paper No. 277 presented at the XXX Colloquium Spectroscopicum Internationale, 21–25 September, Melbourne, Australia, 1997.
7 M. Guilhaus, D. Selby and V. Mlynski, *Mass Spectrom. Rev.*, 2000, **19**, 65.
8 F. Vanhaecke, L. Moens, R. Dams, L. Allen and S. Georgitis, *Anal. Chem.*, 1999, **71**, 3297.
9 X. Tian, H. Emteborg and F. C. Adams, *J. Anal. At. Spectrom.*, 1999, **14**, 1807.
10 H. Emteborg, X. Tian, M. Ostermann, M. Berglund and F. C. Adams, *J. Anal. At. Spectrom.*, 2000, **15**, 239.
11 J. N. Coles and M. Guilhaus, *J. Am. Soc. Mass Spectrom.*, 1994, **5**, 772.
12 A. Montaser, J. A. McLean, H. Liu and J.-M. Mermet, in *Inductively Coupled Plasma Mass Spectrometry*, ed. A. Montaser, Wiley-VCH, New York, 1998, pp. 1–31.
13 I. S. Begley and B. L. Sharp, *J. Anal. At. Spectrom.*, 1994, **9**, 171.
14 G. M. Hieftje, D. P. Myers, G. Li, P. P. Mahoney, T. W. Burgoyne, S. J. Ray and J. P. Guzowski, *J. Anal. At. Spectrom.*, 1997, **12**, 287.
15 K. G. Heumann, S. M. Gallus, G. Radlinger and J. Vogl, *J. Anal. At. Spectrom.*, 1998, **13**, 1001.
16 K. J. R. Rosman and P. D. P. Taylor, *J. Anal. At. Spectrom.*, 1998, **13**, 45N.
17 A. M. Leach, M. Heisterkamp, F. C. Adams and G. M. Hieftje, *J. Anal. At. Spectrom.*, 2000, **15**, 151.